EUROPEAN LABORATORY FOR PARTICLE PHYSICS (CERN)

CERN-PPE/97-122
September 4 1997

Searches for Supersymmetry in the photon(s) plus missing energy channels at $\sqrt{s} = 161$ GeV and 172 GeV

The ALEPH Collaboration*

Abstract

Searches for supersymmetric particles in channels with one or more photons and missing energy have been performed with data collected by the ALEPH detector at LEP. The data consist of 11.1 pb^{-1} at $\sqrt{s} = 161$ GeV, 1.1 pb^{-1} at 170 GeV and 9.5 pb^{-1} at 172 GeV. The $e^+e^- \to \nu\bar{\nu}\gamma(\gamma)$ cross section is measured. The data are in good agreement with predictions based on the Standard Model, and are used to set upper limits on the cross sections for anomalous photon production. These limits are compared to two different SUSY models and used to set limits on the neutralino mass. A limit of 71 GeV/c^2 at 95% C.L. is set on the mass of the lightest neutralino ($\tau_{\chi_1^0} \leq 3$ ns) for the gauge-mediated supersymmetry breaking and LNZ models.

(To be submitted to Physics Letters B)

* See the following pages for the list of authors.

The ALEPH Collaboration

R. Barate, D. Buskulic, D. Decamp, P. Ghez, C. Goy, J.-P. Lees, A. Lucotte, M.-N. Minard, J.-Y. Nief, B. Pietrzyk

Laboratoire de Physique des Particules (LAPP), IN^{2}P^3-CNRS, 74019 Annecy-le-Vieux Cedex, France

M.P. Casado, M. Chmeissani, P. Comas, J.M. Crespo, M. Delfino, E. Fernandez, M. Fernandez-Bosman, Ll. Garrido,[15] A. Juste, M. Martinez, G. Merino, R. Miquel, Ll.M. Mir, C. Padilla, I.C. Park, A. Pascual, J.A. Perlas, I. Riu, F. Sanchez

Institut de Física d'Altes Energies, Universitat Autònoma de Barcelona, 08193 Bellaterra (Barcelona), Spain[7]

A. Colaleo, D. Creanza, M. de Palma, G. Gelao, G. Iaselli, G. Maggi, M. Maggi, N. Marinelli, S. Nuzzo, A. Ranieri, G. Raso, F. Ruggieri, G. Selvaggi, L. Silvestris, P. Tempesta, A. Tricomi,[3] G. Zito

Dipartimento di Fisica, INFN Sezione di Bari, 70126 Bari, Italy

X. Huang, J. Lin, Q. Ouyang, T. Wang, Y. Xie, R. Xu, S. Xue, J. Zhang, L. Zhang, W. Zhao

Institute of High-Energy Physics, Academia Sinica, Beijing, The People's Republic of China[8]

D. Abbaneo, R. Alemany, A.O. Bazarko,[1] U. Becker, P. Bright-Thomas, M. Cattaneo, F. Cerutti, G. Dissertori, H. Drevermann, R.W. Forty, M. Frank, R. Hagelberg, J.B. Hansen, J. Harvey, P. Janot, B. Jost, E. Kneringer, I. Lehraus, P. Mato, A. Minten, L. Moneta, A. Pacheco, J.-F. Pusztaszeri,[20] F. Ranjard, G. Rizzo, L. Rolandi, D. Rousseau, D. Schlatter, M. Schmitt, O. Schneider, W. Tejessy, F. Teubert, I.R. Tomalin, H. Wachsmuth, A. Wagner[21]

European Laboratory for Particle Physics (CERN), 1211 Geneva 23, Switzerland

Z. Ajaltouni, A. Barrès, C. Boyer, A. Falvard, C. Ferdi, P. Gay, C . Guicheney, P. Henrard, J. Jousset, B. Michel, S. Monteil, J-C. Montret, D. Pallin, P. Perret, F. Podlyski, J. Proriol, P. Rosnet, J.-M. Rossignol

Laboratoire de Physique Corpusculaire, Université Blaise Pascal, IN^{2}P^3-CNRS, Clermont-Ferrand, 63177 Aubière, France

T. Fearnley, J.D. Hansen, J.R. Hansen, P.H. Hansen, B.S. Nilsson, B. Rensch, A. Wäänänen

Niels Bohr Institute, 2100 Copenhagen, Denmark[9]

G. Daskalakis, A. Kyriakis, C. Markou, E. Simopoulou, A. Vayaki

Nuclear Research Center Demokritos (NRCD), Athens, Greece

A. Blondel, J.C. Brient, F. Machefert, A. Rougé, M. Rumpf, A. Valassi,[6] H. Videau

Laboratoire de Physique Nucléaire et des Hautes Energies, Ecole Polytechnique, IN^{2}P^3-CNRS, 91128 Palaiseau Cedex, France

T. Boccali, E. Focardi, G. Parrini, K. Zachariadou

Dipartimento di Fisica, Università di Firenze, INFN Sezione di Firenze, 50125 Firenze, Italy

R. Cavanaugh, M. Corden, C. Georgiopoulos, T. Huehn, D.E. Jaffe

Supercomputer Computations Research Institute, Florida State University, Tallahassee, FL 32306-4052, USA [13,14]

A. Antonelli, G. Bencivenni, G. Bologna,[4] F. Bossi, P. Campana, G. Capon, D. Casper, V. Chiarella, G. Felici, P. Laurelli, G. Mannocchi,[5] F. Murtas, G.P. Murtas, L. Passalacqua, M. Pepe-Altarelli

Laboratori Nazionali dell'INFN (LNF-INFN), 00044 Frascati, Italy

L. Curtis, S.J. Dorris, A.W. Halley, I.G. Knowles, J.G. Lynch, V. O'Shea, C. Raine, J.M. Scarr, K. Smith, P. Teixeira-Dias, A.S. Thompson, E. Thomson, F. Thomson, R.M. Turnbull

Department of Physics and Astronomy, University of Glasgow, Glasgow G12 8QQ,United Kingdom[10]

O. Buchmüller, S. Dhamotharan, C. Geweniger, G. Graefe, P. Hanke, G. Hansper, V. Hepp, E.E. Kluge, A. Putzer, J. Sommer, K. Tittel, S. Werner, M. Wunsch

Institut für Hochenergiephysik, Universität Heidelberg, 69120 Heidelberg, Fed. Rep. of Germany[16]

R. Beuselinck, D.M. Binnie, W. Cameron, P.J. Dornan, M. Girone, S. Goodsir, E.B. Martin, P. Morawitz, A. Moutoussi, J. Nash, J.K. Sedgbeer, P. Spagnolo, A.M. Stacey, M.D. Williams

Department of Physics, Imperial College, London SW7 2BZ, United Kingdom[10]

V.M. Ghete, P. Girtler, D. Kuhn, G. Rudolph

Institut für Experimentalphysik, Universität Innsbruck, 6020 Innsbruck, Austria[18]

A.P. Betteridge, C.K. Bowdery, P.G. Buck, P. Colrain, G. Crawford, A.J. Finch, F. Foster, G. Hughes, R.W.L. Jones, T. Sloan, E.P. Whelan, M.I. Williams

Department of Physics, University of Lancaster, Lancaster LA1 4YB, United Kingdom[10]

I. Giehl, C. Hoffmann, K. Jakobs, K. Kleinknecht, G. Quast, B. Renk, E. Rohne, H.-G. Sander, P. van Gemmeren, C. Zeitnitz

Institut für Physik, Universität Mainz, 55099 Mainz, Fed. Rep. of Germany[16]

J.J. Aubert, C. Benchouk, A. Bonissent, G. Bujosa, J. Carr, P. Coyle, C. Diaconu, A. Ealet, D. Fouchez, N. Konstantinidis, O. Leroy, F. Motsch, P. Payre, M. Talby, A. Sadouki, M. Thulasidas, A. Tilquin, K. Trabelsi

Centre de Physique des Particules, Faculté des Sciences de Luminy, IN^{2}P^3-CNRS, 13288 Marseille, France

M. Aleppo, M. Antonelli, F. Ragusa

Dipartimento di Fisica, Università di Milano e INFN Sezione di Milano, 20133 Milano, Italy.

R. Berlich, W. Blum, V. Büscher, H. Dietl, G. Ganis, C. Gotzhein, H. Kroha, G. Lütjens, G. Lutz, W. Männer, H.-G. Moser, R. Richter, A. Rosado-Schlosser, S. Schael, R. Settles, H. Seywerd, R. St. Denis, H. Stenzel, W. Wiedenmann, G. Wolf

Max-Planck-Institut für Physik, Werner-Heisenberg-Institut, 80805 München, Fed. Rep. of Germany[16]

J. Boucrot, O. Callot,[12] S. Chen, A. Cordier, M. Davier, L. Duflot, J.-F. Grivaz, Ph. Heusse, A. Höcker, A. Jacholkowska, M. Jacquet, D.W. Kim,[2] F. Le Diberder, J. Lefrançois, A.-M. Lutz, I. Nikolic, M.-H. Schune, L. Serin, S. Simion, E. Tournefier, J.-J. Veillet, I. Videau, D. Zerwas

Laboratoire de l'Accélérateur Linéaire, Université de Paris-Sud, IN^{2}P^3-CNRS, 91405 Orsay Cedex, France

P. Azzurri, G. Bagliesi,[12] S. Bettarini, C. Bozzi, G. Calderini, V. Ciulli, R. Dell'Orso, R. Fantechi, I. Ferrante, A. Giassi, A. Gregorio, F. Ligabue, A. Lusiani, P.S. Marrocchesi, A. Messineo, F. Palla, G. Sanguinetti, A. Sciabà, G. Sguazzoni, J. Steinberger, R. Tenchini, C. Vannini, A. Venturi, P.G. Verdini

Dipartimento di Fisica dell'Università, INFN Sezione di Pisa, e Scuola Normale Superiore, 56010 Pisa, Italy

G.A. Blair, L.M. Bryant, J.T. Chambers, Y. Gao, M.G. Green, T. Medcalf, P. Perrodo, J.A. Strong, J.H. von Wimmersperg-Toeller

Department of Physics, Royal Holloway & Bedford New College, University of London, Surrey TW20 OEX, United Kingdom[10]

D.R. Botterill, R.W. Clifft, T.R. Edgecock, S. Haywood, P. Maley, P.R. Norton, J.C. Thompson, A.E. Wright

Particle Physics Dept., Rutherford Appleton Laboratory, Chilton, Didcot, Oxon OX11 OQX, United Kingdom[10]

B. Bloch-Devaux, P. Colas, B. Fabbro, W. Kozanecki, E. Lançon, M.C. Lemaire, E. Locci, P. Perez, J. Rander, J.-F. Renardy, A. Rosowsky, A. Roussarie, J.-P. Schuller, J. Schwindling, A. Trabelsi, B. Vallage

CEA, DAPNIA/Service de Physique des Particules, CE-Saclay, 91191 Gif-sur-Yvette Cedex, France[17]

S.N. Black, J.H. Dann, H.Y. Kim, A.M. Litke, M.A. McNeil, G. Taylor

Institute for Particle Physics, University of California at Santa Cruz, Santa Cruz, CA 95064, USA[19]

C.N. Booth, R. Boswell, C.A.J. Brew, S. Cartwright, F. Combley, M.S. Kelly, M. Lehto, W.M. Newton, J. Reeve, L.F. Thompson

Department of Physics, University of Sheffield, Sheffield S3 7RH, United Kingdom[10]

K. Affholderbach, A. Böhrer, S. Brandt, G. Cowan, J. Foss, C. Grupen, G. Lutters, P. Saraiva, L. Smolik, F. Stephan

Fachbereich Physik, Universität Siegen, 57068 Siegen, Fed. Rep. of Germany[16]

M. Apollonio, L. Bosisio, R. Della Marina, G. Giannini, B. Gobbo, G. Musolino

Dipartimento di Fisica, Università di Trieste e INFN Sezione di Trieste, 34127 Trieste, Italy

J. Putz, J. Rothberg, S. Wasserbaech, R.W. Williams

Experimental Elementary Particle Physics, University of Washington, WA 98195 Seattle, U.S.A.

S.R. Armstrong, E. Charles, P. Elmer, D.P.S. Ferguson, S. González, T.C. Greening, O.J. Hayes, H. Hu, S. Jin, P.A. McNamara III, J.M. Nachtman, J. Nielsen, W. Orejudos, Y.B. Pan, Y. Saadi, I.J. Scott, J. Walsh, Sau Lan Wu, X. Wu, J.M. Yamartino, G. Zobernig

Department of Physics, University of Wisconsin, Madison, WI 53706, USA[11]

[1]Now at Princeton University, Princeton, NJ 08544, U.S.A.

[2]Permanent address: Kangnung National University, Kangnung, Korea.

[3]Also at Dipartimento di Fisica, INFN Sezione di Catania, Catania, Italy.

[4]Also Istituto di Fisica Generale, Università di Torino, Torino, Italy.

[5]Also Istituto di Cosmo-Geofisica del C.N.R., Torino, Italy.

[6]Supported by the Commission of the European Communities, contract ERBCHBICT941234.

[7]Supported by CICYT, Spain.

[8]Supported by the National Science Foundation of China.

[9]Supported by the Danish Natural Science Research Council.

[10]Supported by the UK Particle Physics and Astronomy Research Council.

[11]Supported by the US Department of Energy, grant DE-FG0295-ER40896.

[12]Also at CERN, 1211 Geneva 23,Switzerland.

[13]Supported by the US Department of Energy, contract DE-FG05-92ER40742.

[14]Supported by the US Department of Energy, contract DE-FC05-85ER250000.

[15]Permanent address: Universitat de Barcelona, 08208 Barcelona, Spain.

[16]Supported by the Bundesministerium für Bildung, Wissenschaft, Forschung und Technologie, Fed. Rep. of Germany.

[17]Supported by the Direction des Sciences de la Matière, C.E.A.

[18]Supported by Fonds zur Förderung der wissenschaftlichen Forschung, Austria.

[19]Supported by the US Department of Energy, grant DE-FG03-92ER40689.

[20]Now at School of Operations Research and Industrial Engireering, Cornell University, Ithaca, NY 14853-3801, U.S.A.

[21]Now at Schweizerischer Bankverein, Basel, Switzerland.

1 Introduction

The Standard Model (SM) predicts the production of events at LEP2 with one or more photons and missing energy through two processes: radiative returns to the Z resonance ($e^+e^- \to \gamma Z$) with $Z \to \nu\bar{\nu}$, and t-channel W exchange with photon(s) radiated from the beam electrons or the W. Such events have been studied in e^+e^- annihilations at centre-of-mass energies of 130 and 136 GeV [1] and 161 GeV [2] as well as at previous collider experiments [3]. The process $\nu\bar{\nu}\gamma(\gamma)$ is well understood theoretically, so any significant deviation from the predictions of the Standard Model could signal new physics.

Events with one or more photons and missing energy could arise in Supersymmetry where the missing energy is caused by weakly interacting supersymmetric particles. For example, in the Minimal Supersymmetric extension of the Standard Model (MSSM), the second lightest neutralino can decay radiatively to the lightest neutralino [4]. A large branching ratio for this decay is expected only in a small region of parameter space. This region can however be enlarged by breaking the condition on the unification of gaugino masses at the GUT scale.

Alternatively there are SUSY models which postulate that the lightest supersymmetric particle (LSP) is the gravitino. In these models the lightest neutralino decays to an essentially massless gravitino ($M_{\tilde{G}} < 1$ MeV/c^2) and a photon with a 100% branching ratio. Examples include the so-called "No-Scale Supergravity" (LNZ model) [5] and models with gauge-mediated supersymmetry breaking (GMSB) [6, 7, 8, 9, 10]. In both classes of models, one might expect the process $e^+e^- \to \chi_1^0\chi_1^0 \to \tilde{G}\tilde{G}\gamma\gamma$ at LEP2, seen in the detector as two photons and missing energy. The one-photon process $e^+e^- \to \chi_1^0\tilde{G} \to \tilde{G}\tilde{G}\gamma$ is expected to be produced at LEP2 for only very light gravitino masses as the cross section scales as the inverse of the gravitino mass squared [11]. For a gravitino mass of 10^{-5} eV/c^2 the cross section is predicted to be around 1 pb. In the LNZ model the gravitino mass is allowed to be this light [12], but in GMSB the gravitino is predicted to have a mass five orders of magnitude bigger. Thus, this process is not expected in GMSB.

The data collected by ALEPH at energies of 161, 170 and 172 GeV (11.1, 1.1 pb^{-1} and 9.5 pb^{-1}, respectively) have been analysed for anomalous single-photon and two-photon production using criteria optimized for a range of SUSY particle masses. No evidence for anomalous photon(s) and missing energy events is found, and limits are placed on the production of supersymmetric particles in the context of the models introduced above. For GMSB, the neutralino composition is assumed to be pure bino throughout this letter.

The CDF collaboration has observed an unusual event with two high energy electrons, two high energy photons, and a large amount of missing transverse energy [13]. The SM explanation for this event has a low probability, but it can be accommodated by the SUSY models mentioned above. In the neutralino LSP scenario the CDF event could be explained by the Drell-Yan process $q\bar{q} \to \tilde{e}\tilde{e} \to ee\chi_2^0\chi_2^0 \to ee\chi_1^0\chi_1^0\gamma\gamma$ where the two χ_1^0's escape detection resulting in missing transverse energy. If this is the explanation for the CDF event, the best possibility for discovery at LEP2 is $e^+e^- \to \chi_2^0\chi_2^0 \to \chi_1^0\chi_1^0\gamma\gamma$. In principle $e^+e^- \to \chi_2^0\chi_1^0 \to \chi_1^0\chi_1^0\gamma$ could be considered, however the predicted cross section is uninterestingly small. In gravitino LSP models, the CDF event could be explained by $q\bar{q} \to \tilde{e}\tilde{e} \to ee\chi_1^0\chi_1^0 \to ee\tilde{G}\tilde{G}\gamma\gamma$. In this scenario the best channel for discovery at LEP2 is $e^+e^- \to \chi_1^0\chi_1^0 \to \tilde{G}\tilde{G}\gamma\gamma$. The limits derived from the ALEPH data are compared to the regions favored by the CDF event within these models.

The outline of this letter is as follows: after a brief description of the detector in Section 2, the Monte Carlo samples are presented in Section 3, the one photon and two photon plus missing energy searches are detailed in Sections 4 and 5 and conclusions are stated in Section 6.

2 The ALEPH detector and photon identification

The ALEPH detector and its performance are described in detail elsewhere [14, 15]. The analysis presented here depends largely on the performance of the electromagnetic calorimeter (ECAL). The luminosity calorimeters (LCAL and SICAL), together with the hadron calorimeter (HCAL), are used mainly to veto events in which photons are accompanied by other energetic particles. The HCAL is instrumented with streamer tubes, which are useful in identifying muons. The SICAL provides coverage between 34 and 63 mrad from the beam axis while the LCAL provides coverage between 45 and 160 mrad. The LCAL consists of two halves which fit together around the beam axis; the area where the two halves join is a region of reduced sensitivity ('the LCAL crack'). This vertical crack accounts for only 0.05% of the total solid angle coverage of the ALEPH detector. The tracking system, composed of a silicon vertex detector, wire drift chamber (ITC), and time projection chamber (TPC), is used to provide efficient ($> 99.9\%$) tracking of isolated charged particles in the angular range $|\cos\theta| < 0.96$.

The ECAL is a lead/wire-plane sampling calorimeter consisting of 36 modules, twelve in the barrel and twelve in each endcap, which provide coverage in the angular range $|\cos\theta| < 0.98$. Inter-module cracks reduce this solid angle coverage by 2% in the barrel and 6% in the endcaps. However, the ECAL and HCAL cracks are not aligned so there is complete coverage in ALEPH at large polar angles. At normal incidence the ECAL is situated at 185 cm from the interaction point. The total thickness of the ECAL is 22 radiation lengths at normal incidence. Anode wire signals, sampled every 512 ns during their rise time, provide a measurement by the ECAL of the interaction time t_0 of the particles relative to the beam crossing with a resolution better than 15 ns (for showers with energy greater than 1 GeV). Cathode pads associated with each layer of the wire chambers are connected to form projective 'towers', each subtending approximately $0.9^\circ \times 0.9^\circ$, which are oriented towards the interaction point. Each tower is read out in three segments in depth of four, nine and nine radiation lengths. The high granularity of the calorimeter provides excellent identification of photons and electrons. The energy calibration of the ECAL is obtained from Bhabha and gamma-gamma events. The energy resolution is measured to be $\Delta E/E = 0.18/\sqrt{E} + 0.009$ (E in GeV) [15].

Photon candidates are identified using an algorithm [15] which performs a topological search for localised energy depositions within groups of neighboring ECAL towers. These energy depositions are required to have transverse and longitudinal profiles consistent with that of an electromagnetic shower. Photons far from ECAL cracks have their energy measured solely from the localised energy deposition. In order to optimise the energy reconstruction, photons that are not well-contained in the ECAL (near or in a crack) have their energy measured from the sum of the localised energy depositions and all energy deposits in the HCAL within a cone of $\cos\alpha > 0.98$. Photon candidates may also be identified in the tracking system if they convert producing an electron-positron pair [15].

The trigger most relevant for photonic events is the neutral energy trigger. For the 1996 run, the total wire energy measured in an ECAL module must be greater than 1 GeV in the barrel and 2.3 GeV in the endcaps in order for this trigger to fire. The neutral energy trigger is fully efficient for the analyses to be described.

3 The Monte Carlo samples

The efficiency for the $e^+e^- \to \nu\bar{\nu}\gamma(\gamma)$ cross section measurement and the background for the anomalous photon plus missing energy searches are estimated using the KORALZ Monte Carlo program [16]. This Monte Carlo is checked by comparing to NUNUGG [17] at $\sqrt{s}$ below the W threshold and to CompHEP [18] at higher energies. The Monte Carlos agree within errors to 1% for the emission of one photon. The two photon plus missing energy signature is checked for loose acceptance cuts ($E_\gamma > 5\,\mathrm{GeV}$, $|\cos\theta| < 0.95$) and in a more restrictive region ($\mathrm{Missing\,Mass} > 100\,\mathrm{GeV}/c^2$). The discrepancy between KORALZ and CompHEP is at most 10% [19] .

Background to the photon(s) plus missing energy signature can come from $e^+e^- \to \gamma\gamma(\gamma)$ and $e^+e^- \to e^+e^-$ where initial or final state particles radiate a photon and the final state particles escape along the beam direction undetected. This background is studied using the GGGB03 [20] and BHWIDE [21] Monte Carlo programs, respectively. The signal generator SUSYGEN [22] is used to design the selection criteria and evaluate the efficiency for the searches for new physics.

4 One photon and missing energy

The Standard Model predicts a large cross section for the process $e^+e^- \to \nu\bar{\nu}\gamma(\gamma)$, which constitutes an irreducible background to searches for new physics. One can, however, still search for new physics by observing an excess of events over the Standard Model prediction. This requires a precise understanding of the background level from $e^+e^- \to \nu\bar{\nu}\gamma(\gamma)$ and a reduction of cosmic ray and detector noise events (non-subtractable backgrounds) to a negligible level.

4.1 Event selection

Initially, events are selected with no charged tracks (not coming from a conversion) and exactly one photon inside the acceptance cuts of $|\cos\theta| < 0.95$ and $p_\perp > 0.0375\sqrt{s}$ (where $p_\perp$ is defined as the measured transverse momentum relative to the beam axis). The remaining selection criteria are tailored to eliminate as much as possible the non-subtractable backgrounds. Cosmic ray events that traverse the detector are eliminated by the charged track requirement or if there are hits in the outer part of the HCAL. A small fraction of cosmic ray events and detector noise events in the ECAL remain after these cuts. The ECAL information can be exploited to remove these types of events. The barycentre of the photon shower is found in each of the three ECAL stacks. Taking two points at a time, three possible photon trajectories are calculated and used to estimate the distance of closest approach of the photon to the interaction point. The smallest of the three distances ('impact parameter of the photon') is required to be less than 25 cm. The compactness of the shower in the ECAL is calculated by taking an energy-weighted average of the angle subtended at the interaction point between the cluster barycentre and the barycentre of each of the ECAL storeys contributing to the cluster. The compactness is required to be less than 0.85°. Both the impact parameter and compactness distributions are peaked at low values for photons coming from the interaction point and at high values for the remaining background. The cuts are chosen so that there is negligible efficiency loss for real photons. Finally, the interaction time is required to be within 40 ns of the beam crossing.

A single photon and missing energy might also be caused by initial or final state radiation when the final state particles escape along the beam direction. Most of the events that satisfy the requirement that the $p_\perp$ of the photon must be greater than $0.0375\sqrt{s}$ will have a particle

Selection	Efficiency(%)	
	161 GeV	172 GeV
$N_\gamma \geq 1$ and $N_{ch} = 0$	94	94
$N_\gamma = 1$	89	89
$p_\perp > 0.145\sqrt{s}$ if $\phi_{pmiss} = 90 \pm 17$ or 270 ± 17	82	82
Additional energy < 1 GeV	72	74
No energy within 14° of the beam axis	71	73
All other cuts	70	72

Table 1: *The cumulative efficiency for the* $e^+e^- \to \nu\bar{\nu}\gamma(\gamma)$ *process inside the acceptance cuts.*

within the angular acceptance of the detector. These events are eliminated by the no charged track requirement and the following cut. The event is rejected if the total energy in the detector excluding the photon is more than 1 GeV or if there is any energy reconstructed within 14° of the beam axis. This requirement reduces the efficiency for $e^+e^- \to \nu\bar{\nu}\gamma(\gamma)$ by 11% due to additional brehmsstrahlung photons at low angles (7% loss) and uncorrelated noise in the detector (4% loss). To compensate for vertical cracks in the LCAL, the $p_\perp$ requirement is tightened to $0.145\sqrt{s}$ if the missing momentum vector points to within 17° of 90° or 270° in azimuthal angle (ϕ).

Residual cosmic ray and detector noise backgrounds are measured by selecting events slightly out of time with respect to the beam crossing but which pass all other cuts. No such events are found in a displaced time window of 740 ns width. Events with a radiated photon in the acceptance and the final state particles escaping undetected along the beam axis are studied using Monte Carlo. The equivalent of 60 data sets of these SM background processes was generated and passed through the full detector simulation. No events from these samples survive the selection.

4.2 Measurement of the $e^+e^- \to \nu\bar{\nu}\gamma(\gamma)$ cross section

The efficiency for the process $e^+e^- \to \nu\bar{\nu}\gamma(\gamma)$ is detailed in Table 1. The efficiency loss due to uncorrelated noise or beam-related background in the detector is estimated using events triggered at random beam crossings and is included in the efficiency estimate. Applying the selection criteria to the data, 41 one-photon events are found at $\sqrt{s} =$ 161 GeV while 45 are expected from Monte Carlo. At $\sqrt{s} = 170/172$ GeV, 36 one-photon events are found while 37 are expected.

Inside the acceptance $|\cos\theta| < 0.95$ and $p_\perp > 0.0375\sqrt{s}$ the cross section measurements are

$$\sigma(e^+e^- \to \nu\bar{\nu}\gamma(\gamma)) = 5.3 \pm 0.8 \pm 0.2\,\text{pb} \qquad \sqrt{s} = 161\,\text{GeV}$$

$$\sigma(e^+e^- \to \nu\bar{\nu}\gamma(\gamma)) = 4.7 \pm 0.8 \pm 0.2\,\text{pb} \qquad \sqrt{s} = 172\,\text{GeV}.$$

These results are consistent with the Standard Model predictions of 5.81 ± 0.03 pb at 161 GeV and 4.85 ± 0.04 pb at 172 GeV obtained using the KORALZ Monte Carlo. The missing mass and polar angle distributions are shown in Figure 1.

The estimates of the systematic uncertainties in the above cross sections include contributions from the sources listed in Table 2. The simulation of the energetic photon shower is checked with a sample of Bhabha events selected requiring two collinear beam-momentum tracks and using muon chamber information to veto $\mu^+\mu^-$ events. The tracking information was masked from these events and the photon reconstruction redone. The efficiency to reconstruct a photon in these events is found to be consistent within the available statistics at the 3% level. The uncertainty

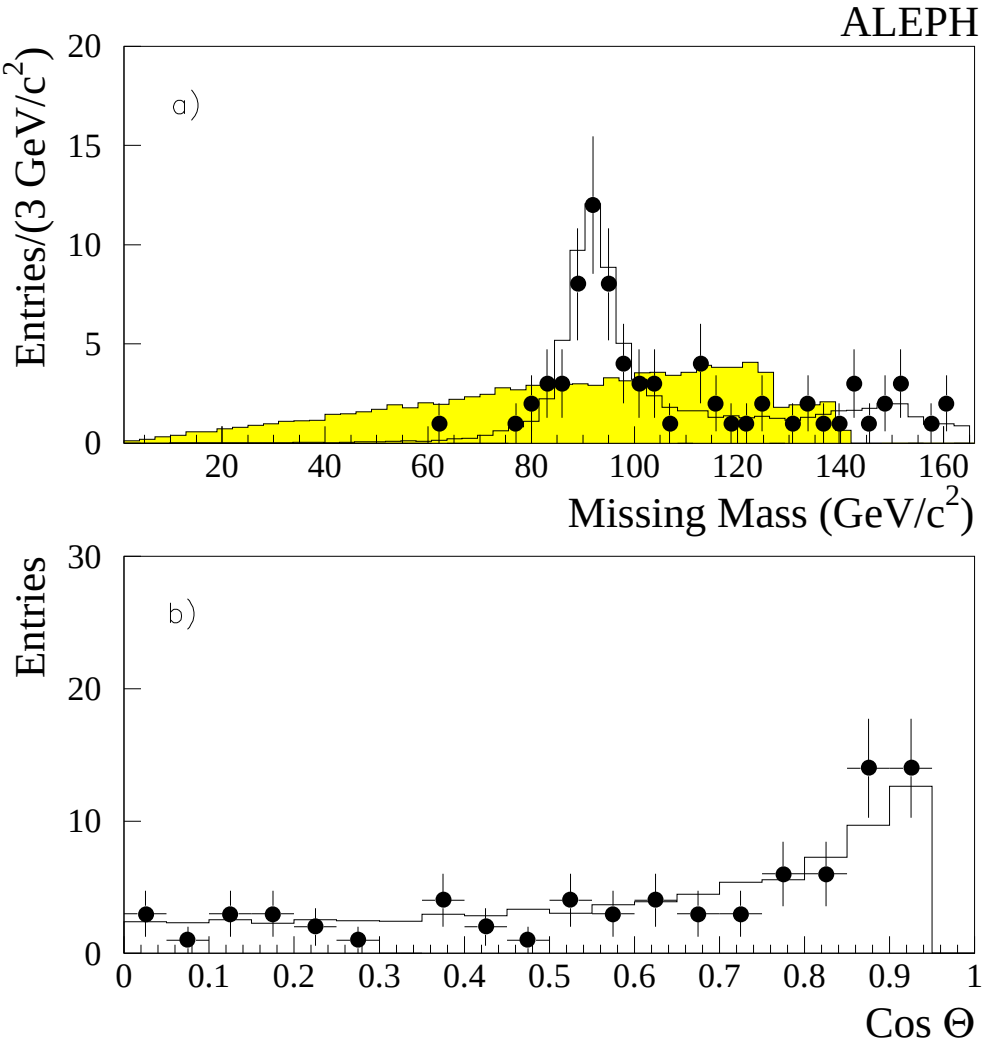

Figure 1: *a) The invariant mass distribution of the system recoiling against the photon candidate is shown for both the data (points with error bars) and Monte Carlo (histogram). The signal* $e^+e^- \to \chi_1^0\tilde{G} \to \tilde{G}\tilde{G}\gamma$ *for a* χ_1^0 *mass of 100 GeV/*c^2 *is overlaid (shaded histogram) with arbitrary normalization. b) The* $\cos\theta$ *distribution is shown for both the data (points with error bars) and Monte Carlo (histogram). The signal has a flat distribution in* $\cos\theta$*.*

in the number of simulated pair conversions is estimated to give a 0.3% change in the overall efficiency. To account for the uncertainty in the energy calibration the energy is shifted by 2% and the efficiency is recalculated. The difference in the efficiency is found to be 0.2%. The total systematic uncertainty is obtained by adding in quadrature the individual contributions.

4.3 Search for a light gravitino in the one-photon channel

In order to search for the signal $e^+e^- \to \chi_1^0\tilde{G} \to \tilde{G}\tilde{G}\gamma$, a binned maximum likelihood fit is performed on the observed missing mass spectrum under the hypothesis that there is a mixture

Source	Error(%)
Photon selection	3
Converted photon selection	0.3
Energy calibration	0.2
Background	<1
Integrated luminosity	0.7
Monte Carlo theoretical	1
Monte Carlo statistical	0.4
Total (in quadrature)	4

Table 2: *Systematic uncertainties for the one-photon channel.*

of signal and background in the data. Events from the $e^+e^- \to \nu\bar{\nu}\gamma(\gamma)$ and $e^+e^- \to \chi_1^0\tilde{G} \to \tilde{G}\tilde{G}\gamma$ processes have very different missing mass distributions, as shown in Figure 1. The likelihood that the missing mass distribution of the data agrees with the composite missing mass distributions of the Monte Carlo background $e^+e^- \to \nu\bar{\nu}\gamma(\gamma)$ and signal $e^+e^- \to \chi_1^0\tilde{G} \to \tilde{G}\tilde{G}\gamma$ processes is calculated. Following the method of Ref. [23], the upper limit on the total number of signal events S is calculated by integrating the likelihood as a function of S. The number of expected signal events is increased until the integration from $S = 0$ to μ_S is 95% of the total area (the integration from $S = 0$ to ∞). The upper limit on the total number of signal events at the 95% confidence level is then given by μ_S. This procedure is repeated at each neutralino mass ranging from 40 GeV/c^2 to 171 GeV/c^2 in steps of 1 GeV/c^2.

A toy Monte Carlo with the kinematic cuts applied is used to describe the signal shape of the missing mass distribution for each neutralino mass. The MC is used to estimate the efficiency loss due to initial state radiation and photon reconstruction. The efficiency loss due to noise in the detector is also included.

The upper limit on the cross section at 95% confidence level is shown in Figure 2. A negligible neutralino lifetime is assumed. The luminosity of the two data samples is combined assuming β^8 threshold dependence of the cross section. The systematic uncertainty is taken into account following Ref. [24], which changes the upper limit on the number of signal events by less than 1%. In the LNZ theory [12], for a gravitino mass of 10^{-5} eV/c^2, the mass limit for the neutralino is 100 GeV/c^2. However, the cross section for this process scales as the inverse of the gravitino mass squared, so the limit on the neutralino mass is very sensitive to the assumed gravitino mass.

5 Two photons and missing energy

As described in the introduction, there are two SUSY scenarios which can give acoplanar photons: the gravitino LSP and neutralino LSP scenarios. The signals differ in that the invisible particle is essentially massless in the first scenario and can have substantial mass in the second one. This leads to two slightly different search criteria, as described in the subsections below.

The cross section for the SM background process $\nu\bar{\nu}\gamma\gamma$ is reduced by order α from the single-photon cross section, so a cut-based analysis is sufficient to search for new physics. The preselection begins by requiring no charged tracks that do not come from a conversion. Due to detector acceptance only photons within $|\cos\theta| < 0.95$ are counted. Since at least two photons are required, background from cosmic rays and detector noise is less severe, so the impact parameter requirement

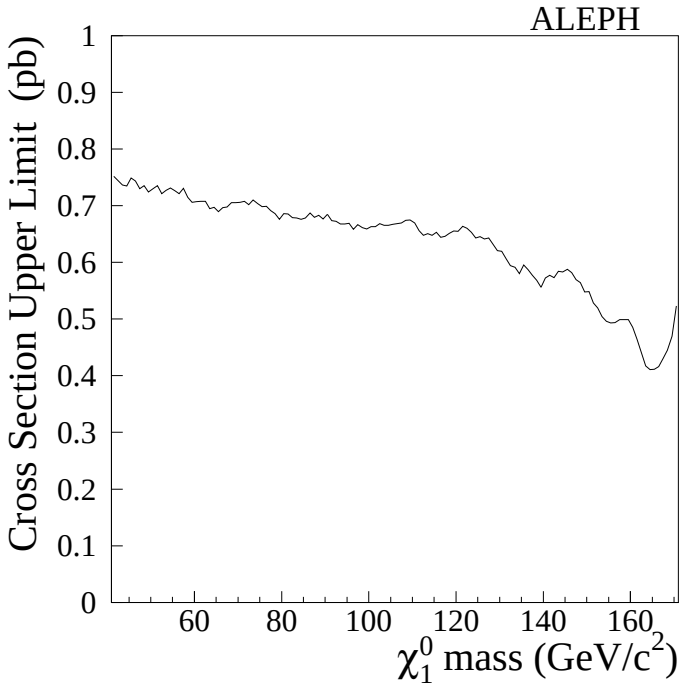

Figure 2: *The 95% C.L. upper limit on the production cross-section for* $e^+e^- \to \chi_1^0\tilde{G} \to \tilde{G}\tilde{G}\gamma$. *The limit is valid for* $\sqrt{s} = 172$ *GeV assuming* β^8 *threshold dependence and isotropic decays.*

is not imposed. Events with more than two photons are required to have at least $0.4\sqrt{s}$ of missing energy. Missing transverse energy is required by imposing an acoplanarity cut at 177° and requiring that the additional total energy be less than 1 GeV. When there are three or more photons in the event, the two most energetic photons are used to determine the acoplanarity. The $e^+e^- \to \gamma\gamma(\gamma)$ background is effectively eliminated after these selection criteria. The total $p_\perp$ is required to be greater than 3.75% of the missing energy, reducing background from radiating events with final state particles escaping down the beam-axis to a negligible level. The selection criteria are shown in Table 3. After this initial selection, two events are selected at 161 GeV while 2.7 are expected from $e^+e^- \to \nu\bar{\nu}\gamma(\gamma)$. At 172 GeV, one event is selected while 2.3 are expected.

5.1 Acoplanar photon search: gravitino LSP scenario

An additional cut is placed on the energy of the less energetic photon (E_2) to reduce substantially the remaining SM background. The energy distribution of the second most energetic photon is peaked near zero for the background, whereas for the signal both photons have a flat distribution in an interval depending on the neutralino mass and $\sqrt{s}$. The theoretical cross section for a pure bino neutralino is used to estimate the expected limit on the neutralino mass. The cut is placed according to the $\bar{N}_{95}$ optimisation procedure [25] at $E_2 < 18$ GeV, reducing the background to 43 fb, while the efficiency remains high at 69% for a neutralino of 65 GeV/c^2 mass produced at 161 GeV. After this selection criteria no events are found in the data while 0.92 events are expected from background processes. Figure 3 shows the upper limit on the cross section compared to two theoretical predictions. The integrated luminosity taken at $\sqrt{s} = 161$ GeV is scaled by the ratio

Two-photon selection criteria	Cumulative signal eff.(%)	$\nu\bar{\nu}\gamma\gamma(\gamma)$ bkg. σ (pb)	$\gamma\gamma(\gamma)$ bkg. σ (pb)
N_γ=2 OR ($N_\gamma \geq 3$ and $E_{missing} > 0.4\sqrt{s}$)	83	0.36	11.9
Acoplanarity $< 177°$	81	0.35	0.3
Additional energy < 1 GeV	73	0.32	0.008
Total $p_\perp > 0.0375 * E_{missing}$	73	0.30	0.002
$\underline{\tilde{G}\text{ LSP analysis}}$			
$E_2 \geq 18$ GeV	69	0.043	0.002
$\underline{\chi_1^0\text{ LSP analysis}}$			
$M_{missing} \leq 82$ GeV/c^2 OR $M_{missing} \geq 100$ GeV/c^2	71	0.16	0.002
OR $E_2 \geq 10$ GeV			
Two photons inside $\lvert\cos\theta\rvert < 0.8$	52	0.063	-

Table 3: *Two-photon selection criteria, and the additional cuts required by the two analyses described in the text. Signal efficiency for the gravitino LSP analysis is given for a 65 GeV/c^2 χ_1^0 at $\sqrt{s} = 161$ GeV. For the χ_1^0 LSP analysis the efficiency numbers are given for a 45 GeV/c^2 χ_2^0 and a 20 GeV/c^2 χ_1^0. Background numbers are given for $\sqrt{s} = 161$ GeV but are similar for 172 GeV.*

of cross sections to those at 172 GeV. The neutralino is taken to be pure bino and the right-selectron mass is set to 1.5 the neutralino mass. The upper limit on the cross section is not strongly dependent on the above choices. Scaling the luminosity at 161 GeV by the threshold dependence β^3/s changes the cross section limit by less then 5%. The mass limit obtained for both the GMSB and LNZ models is

$$M_{\chi_1^0} \geq 71\,\mathrm{GeV/c^2}$$

at 95% C.L. for a neutralino with $\tau_{\chi_1^0} \leq 3$ ns. The analysis is efficient as long as the χ_1^0 decays inside the ECAL. The systematic uncertainty for this analysis is less than 6%, dominated by photon reconstruction efficiency. The effect of this uncertainty on the cross section upper limit is less then 1%, taken into account by means of the method of Ref. [24]. The effect on the mass limit is negligible.

In the GMSB model the neutralino can have a non-negligible lifetime which depends directly on the SUSY breaking scale $\sqrt{F}$. The lifetime of the neutralino is given by [6]

$$c\tau \simeq 130 \left(\frac{100\,\mathrm{GeV/c^2}}{M_{\chi_1^0}}\right)^5 \left(\frac{\sqrt{F}}{100\,\mathrm{TeV}}\right)^4 \mu\mathrm{m}.$$

For a neutralino of mass 71 GeV/c^2 and lifetime 3 ns, the SUSY breaking scale is 600 TeV. Figure 4 shows the 95% C.L. exclusion limit in the $\sqrt{F}$, $M_{\chi_1^0}$ plane.

At LEP2 the production of bino neutralinos would proceed via t-channel selectron exchange. Right-selectron exchange dominates over left-selectron exchange. Thus, the cross section for $e^+e^- \to \chi_1^0\chi_1^0$ depends strongly on the right-selectron mass. The theoretical cross section for $e^+e^- \to \chi_1^0\chi_1^0$ is calculated at each $M_{\tilde{e}_R}$, $M_{\chi_1^0}$ mass point for right-selectron masses ranging from

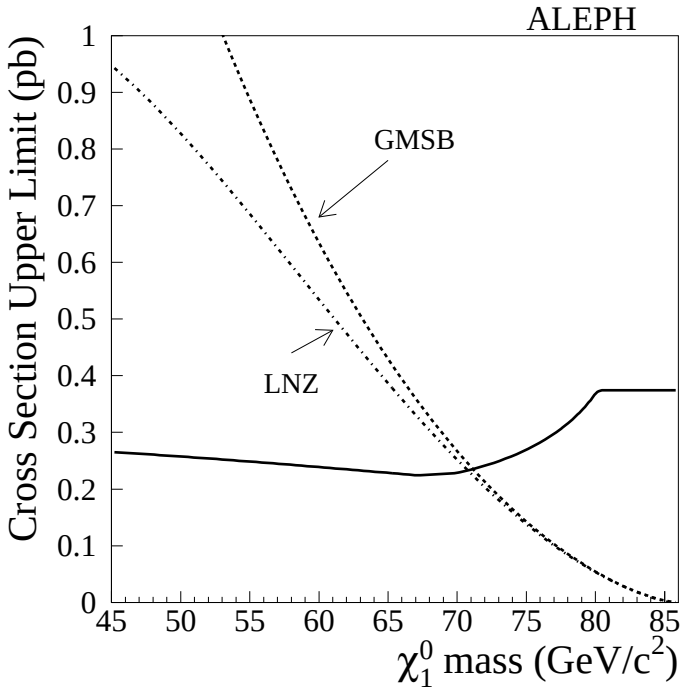

Figure 3: *The 95% C.L. upper limit on the production cross section for* $e^+e^- \to \chi_1^0\chi_1^0 \to \tilde{G}\tilde{G}\gamma\gamma$ *when* χ_1^0 *has a lifetime less than 3 ns. The limit is valid for* $\sqrt{s}$ *= 172 GeV. The data from 161 GeV are included by scaling the luminosity by the ratio of the cross section at that energy to the cross section at 172 GeV. Two different theories are compared to the experimental limit. The right selectron mass is taken to be 1.5 that of the neutralino mass for the GMSB Theory.*

70 GeV/c^2 to 200 GeV/c^2 and neutralino masses ranging from 30 GeV/c^2 to 86 GeV/c^2 and compared to the experimental limit to obtain the exclusion region. The neutralino mass limits were also checked for various left-selectron masses. The result is found to be robust at the ± 1 GeV/c^2 level for left-selectron masses ranging from $M_{\tilde{e}_L} = M_{\tilde{e}_R}$ to $M_{\tilde{e}_L} \gg M_{\tilde{e}_R}$.

The experimentally excluded region in the neutralino, selectron mass plane is shown in Figure 5. Overlayed is the 'CDF region', the area in the neutralino, selectron mass plane where the properties of the CDF event are compatible with the process $q\bar{q} \to \tilde{e}\tilde{e} \to ee\chi_1^0\chi_1^0 \to ee\tilde{G}\tilde{G}\gamma\gamma$. Half of the CDF region is excluded at 95% C.L. by this analysis.

5.2 Acoplanar photon search: neutralino LSP scenario

For the neutralino LSP scenario, a simple energy cut is not optimal since the χ_1^0 is massive and the photons from the $\chi_2^0 \to \chi_1^0\gamma$ decay can have low energy. Here the fact that the $\nu\bar{\nu}\gamma\gamma(\gamma)$ background peaks at small polar angles and has a missing mass near the Z mass is utilised. Events that have missing mass between 82 GeV/c^2 and 100 GeV/c^2, and the energy of the second most energetic photon less than 10 GeV are rejected. The $\cos\theta$ cut is optimised by using the $\bar{N}_{95}$ procedure, leading to a requirement of $|\cos\theta| < 0.8$. The efficiency for various χ_2^0 and χ_1^0 masses is shown in Table 4.

One event is found in the data while 1.3 events are expected from background. The upper

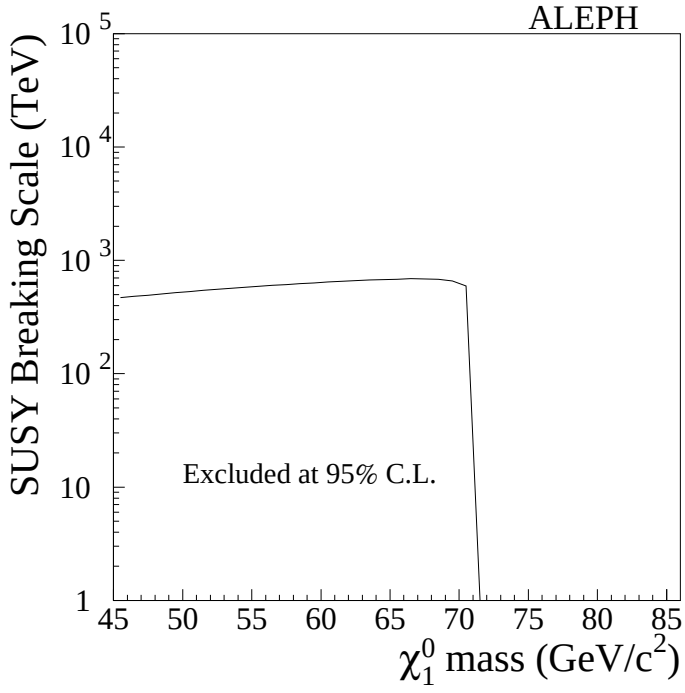

Figure 4: *The excluded region in the neutralino mass, $\sqrt{F}$ plane, where the selectron mass is set to 1.5 times the neutralino mass and the neutralino composition is pure bino.*

	$M_{\chi_2^0-\chi_1^0}$ (GeV/c^2)			
$M_{\chi_2^0}$ (GeV/c^2)	5	10	20	40
5	33			
10	41	45		
40	40	51	51	52
80	34	47	55	57

Table 4: *The efficiency(%) for the* $e^+e^- \to \chi_2^0\chi_2^0 \to \chi_1^0\chi_1^0\gamma\gamma$ *process at* $\sqrt{s} = 161\,\mathrm{GeV}$. *The efficiencies at 172 GeV are equal to (within errors) those at 161 GeV.*

limit on the cross section in the χ_1^0, χ_2^0 mass plane are shown in Figure 6, assuming a branching ratio for $\chi_2^0 \to \chi_1^0\gamma$ of 100%. The systematic uncertainties for this analysis are the same as for the gravitino LSP scenario and the effect on the upper limit is again less than 1%.

The χ_1^0 LSP interpretation of the CDF event (along with the non-observation of other SUSY signatures at Fermilab) suggests a high branching ratio for $\chi_2^0 \to \chi_1^0\gamma$. A 100% branching ratio is achieved when the χ_2^0 is pure photino and the χ_1^0 is pure higgsino. Assuming this scenario, the lower mass limit of χ_2^0 as a function of the selectron mass is calculated and compared to the region compatible with the CDF event. In Figure 7 two scenarios $M_{\tilde{e}_L} = M_{\tilde{e}_R}$ and $M_{\tilde{e}_L} \gg M_{\tilde{e}_R}$ are shown. With the assumption that the χ_2^0 is pure photino and the χ_1^0 is pure higgsino, these results exclude a significant portion of the region compatible with the kinematics of the CDF event given by the neutralino LSP interpretation.

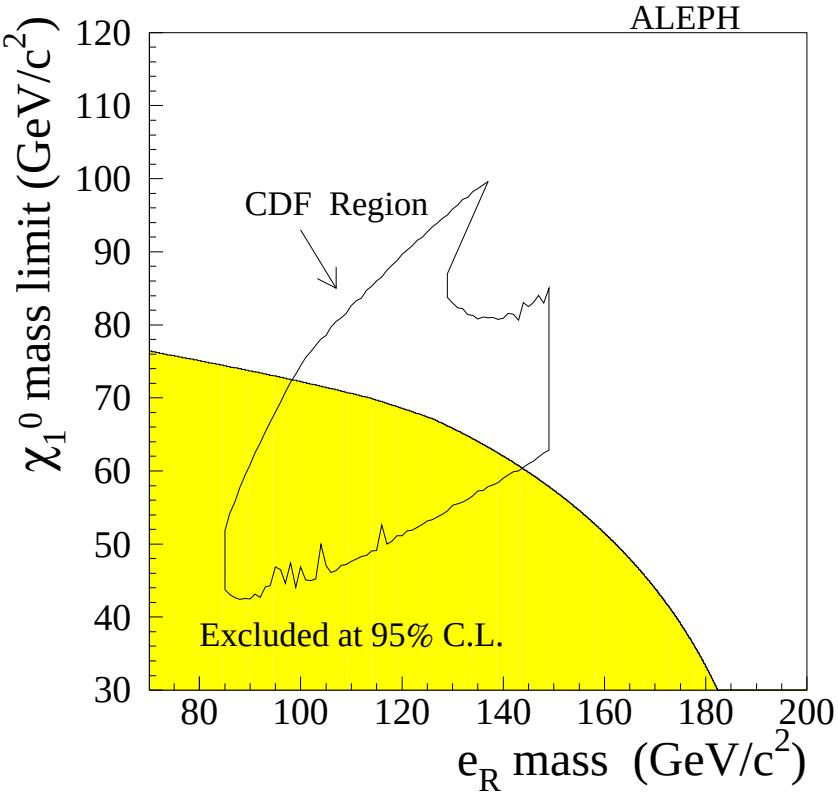

Figure 5: *The excluded region in the neutralino, selectron mass plane at 95% C.L. for a pure bino neutralino (shaded area). Overlayed is the CDF region determined from the properties of the CDF event assuming the reaction* $q\bar{q} \to \tilde{e}\tilde{e} \to ee\chi_1^0\chi_1^0 \to ee\tilde{G}\tilde{G}\gamma\gamma$ *(taken from the Ref. [5]).*

6 Conclusion

Data recorded with the ALEPH detector at LEP centre-of-mass energies of 161 GeV and 170/172 GeV show no signs of new physics in the photon(s) plus missing energy channels. The cross sections and distributions for $e^+e^- \to \nu\bar{\nu}\gamma(\gamma)$ are measured and found to be in agreement with Standard Model expectations. The experimental 95% C.L. upper limits on the cross sections are derived for the following supersymmetric processes $e^+e^- \to \chi_1^0\tilde{G} \to \tilde{G}\tilde{G}\gamma$, $e^+e^- \to \chi_1^0\chi_1^0 \to \tilde{G}\tilde{G}\gamma\gamma$ and $e^+e^- \to \chi_2^0\chi_2^0 \to \chi_1^0\chi_1^0\gamma\gamma$. These cross section limits are actually more general and can be applied to the reactions: $e^+e^- \to XY \to YY\gamma$ where Y is massless and $e^+e^- \to XX \to YY\gamma\gamma$ where Y is massless or has mass. The 95% C.L. limit on the χ_1^0 mass is found to be 71 GeV/c^2 ($\tau_{\chi_1^0} \leq 3$ ns) for gravitino LSP SUSY scenarios. The excluded region of the SUSY Breaking Scale as a function of neutralino mass is derived. The lower limit on the χ_1^0 (χ_2^0) mass as a function of selectron mass is determined and compared to the region compatible with the CDF event for the gravitino (neutralino) LSP scenario.

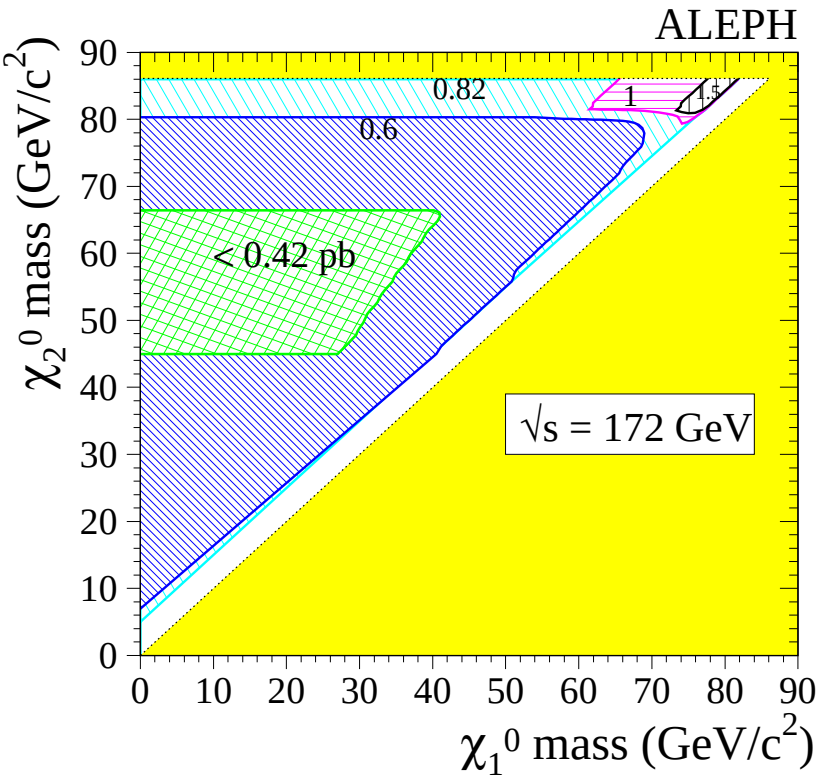

Figure 6: *The 95% C.L. upper limit on the production cross section for* $e^+e^- \to \chi_2^0\chi_2^0 \to \chi_1^0\chi_1^0\gamma\gamma$ *multiplied by the* $BR(\chi_2^0 \to \chi_1^0\gamma)$ *squared. The limit is valid for* $\sqrt{s} = 172$ *GeV assuming* β *threshold behavior and isotropic decays.*

Acknowledgements

Fruitful discussions with Gian Giudice are gratefully acknowledged. We wish to congratulate our colleagues in the CERN accelerator divisions for the successful startup of the LEP2 running. We are grateful to the engineers and technicians in all our institutions for their contribution towards the excellent performance of ALEPH. Those of us from non-member countries thank CERN for its hospitality.

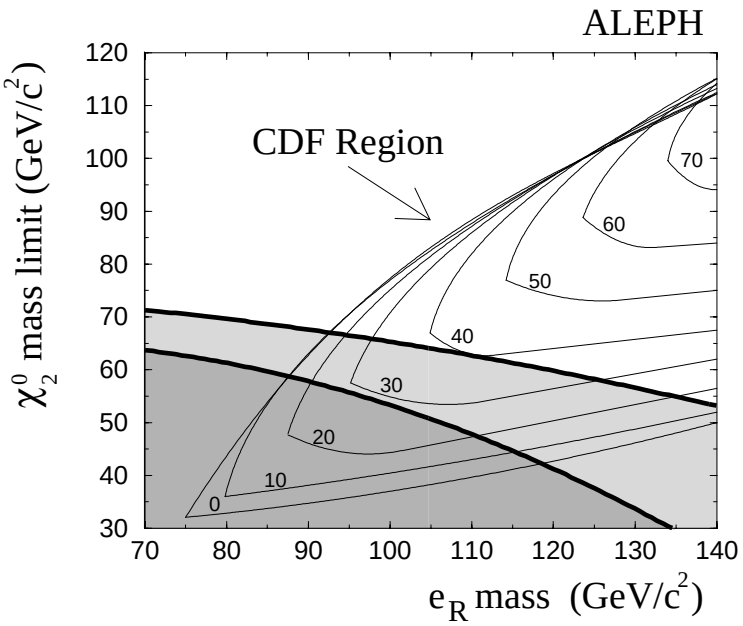

Figure 7: *The excluded region in the neutralino, selectron mass plane at 95% C.L. The* χ_2^0 *is pure photino and the* χ_1^0 *is pure higgsino which implies* $BR(\chi_2^0 \to \chi_1^0\gamma) = 1$. *The shaded area is for* $M_{\tilde{e}_L} = M_{\tilde{e}_R}$. *The darker shaded region refers to* $M_{\tilde{e}_L} \gg M_{\tilde{e}_R}$. *The mass limit is independent of the* χ_1^0 *mass as long as* $\Delta M \geq 25$ *GeV/*c^2. *Overlayed is the CDF region labeled by the mass of* χ_1^0 *in GeV/*c^2. *This is the area determined from the properties of the CDF event assuming the reaction* $q\bar{q} \to \tilde{e}\tilde{e} \to ee\chi_2^0\chi_2^0 \to ee\chi_1^0\chi_1^0\gamma\gamma$ *(taken from Ref. [26]).*

References

[1] ALEPH Collaboration, Phys. Lett. **B384** (1996) 333;
DELPHI Collaboration, Phys. Lett. **B380** (1996) 471;
L3 Collaboration, Phys. Lett. **B384** (1996) 323;
OPAL Collaboration, Phys. Lett. **B377** (1996) 222.

[2] OPAL Collaboration, Phys. Lett. **B391** (1997) 210;
L3 Collaboration, CERN-PPE/97-76, submitted to Phys. Lett. **B**.

[3] JADE Collaboration, W. Bartel et al., Phys. Lett. **B139** (1984) 327;
CELLO Collaboration, H. J. Behrend et al., Z. Phys. **C35** (1987) 181;
VENUS Collaboration, K. Abe et al., Z. Phys **C45** (1989) 175;
ASP Collaboration, G. Bartha et al., Phys. Rev. **D39** (1989) 3207.

[4] H. Haber and D. Wyler, Nucl. Phys. **B323** (1989) 267.

[5] J. Lopez and D. Nanopoulos, Phys. Rev. **D55** (1997) 4450.

[6] S. Dimopoulos et al., Phys. Rev. Lett. **76** (1996) 3494.

[7] S. Dimopoulos, S. Thomas and J. D. Wells, Nucl. Phys. **B488** (1997) 39.

[8] M. Dine, W.Fischler and M. Srednichi, Nucl. Phys. **B189** (1981) 575.

[9] M. Dine, A. Nelson and Y. Shirman, Phys. Rev. **D51** (1995).

[10] P. Fayet, Phys. Lett. B69 (1977) 489, **B70** (1977) 461.

[11] P. Fayet, Phys. Lett. **B175** (1986) 471.

[12] J. Lopez and D. Nanopoulos, Phys. Rev. **D55** (1997) 5813.

[13] S. Park, in Proceedings of the 10th Topical Workshop on Proton-Antiproton Collider Physics, Fermilab, 1995, edited by R. Raja and J. Yoh (AIP, New York, 1995), p 62.

[14] ALEPH Collaboration, Nucl. Instrum. Methods **A294** (1990) 121.

[15] ALEPH Collaboration, Nucl. Instrum. Methods **A360** (1995) 481.

[16] S. Jadach, B.F.L. Ward and Z. Was, Comp. Phys. Commun. **79** (1994) 503.

[17] R. Miquel, C.Mana and M. Martinez, Z. Phys. **C48** (1990) 309.

[18] E. Boss et al., hep-ph/9503280

[19] DELPHI Collaboration, Proceedings of HEP'97 Conference, Jerusalem, 1997.

[20] F.A. Berends and R. Kleiss, Nucl. Phys. **B186** (1981) 22.

[21] S. Jadach, W. Placzek and B. F. L. Ward, preprint UTHEP-95-1001 (unpublished).

[22] S. Katsanevas and S. Melachroinos, in *Physics at LEP2*, Eds. G. Altarelli, T. Sjöstrand, F. Zwirner, CERN Report 96-01, Volume 2 (1996) 328.

[23] V. Innocente and L. Lista, Nucl. Instrum. Methods **A340** (1994) 396;
T. Bayes, Philosophical Transactions of the Royal Society **53** (1763) 370, reprinted in Biometrika 45 (1958) 159.

[24] R. D. Cousins and V. L. Highland, Nucl. Instrum. Methods **A320** (1992) 331.

[25] ALEPH Collaboration, Phys. Lett. **B384** (1996) 427.

[26] S. Ambrosanio et al., Phys. Rev. **D55** (1997) 1372.